

# Evaluation of Longitudinal Strength of a Cargo Barge Based on Shear Force and Still Water Bending Moment under Various Loading Conditions

Budhi Santoso<sup>1\*</sup>, Romadhoni<sup>1</sup>, Jamal<sup>1</sup>, Nauval Abdurahman P<sup>2</sup>, Deny Nusyirwan<sup>3</sup>, Zulfaidah Ariany<sup>4</sup>

<sup>1</sup>Department of Naval Architecture, Polytecnic State of Bengkalis, Sei. Alam, Bengkalis – Riau 28711, Indonesia

<sup>2</sup>Marine Engineering Technology Study Program, Batam State Polytechnic. Jl. Ahmad Yani, Tering Road, Batam Kota District, Batam City, Riau Islands 29461, Indonesia

<sup>3</sup>Marine Engineering Study Program, Faculty of Maritime Engineering and Technology, Raja Ali Haji Maritime University, 29111 Indonesia

<sup>4</sup>Department of Industrial Technology, Vocational College, Universitas Diponegoro, Semarang, 50275, Indonesia

## KEYWORDS

*Cargo barge;  
Hull girder response;  
Loading condition;  
Longitudinal strength;  
Shear force.*

**ABSTRACT** – Longitudinal strength is a fundamental aspect of barge structural safety because variations in loading magnitude and load position may significantly affect the global hull girder response. This study evaluates the longitudinal strength of a cargo barge based on shear force and still water bending moment under several loading conditions, with reference to the applicable BKI Rules for longitudinal strength assessment. The object of the study is a cargo barge with principal dimensions of 330 ft × 90 ft × 21 ft and a lightship weight of 1802.9 metric tons. Six loading conditions were investigated, namely lightship, fully loaded, partially loaded at 50% with homogeneously distributed cargo, and three crane-shift positions at the aft, midship, and fore sections. The net load distribution was obtained from the difference between distributed weight and buoyancy, and then integrated to determine the shear force and still water bending moment along the hull. The results show that the fully loaded condition produced the most critical structural response, with a maximum shear force of  $0.385 \times 10^3$  metric tons at Frame 50 and a maximum still water bending moment of  $-6.212 \times 10^3$  metric ton·m at Frame 35, indicating a dominant sagging condition. The governing case reached only 32.49% of the allowable shear force and 33.58% of the allowable still water bending moment, confirming a substantial safety margin. The crane-shift analysis further demonstrates that movable concentrated loads can shift critical internal force locations, which may be overlooked in standard cargo distribution analysis. All evaluated loading conditions remained below the permissible limits, indicating that the barge is structurally acceptable under the investigated still-water loading scenarios.

\*Corresponding Author | Author | ✉ ([budhisantoso@polbeng.ac.id](mailto:budhisantoso@polbeng.ac.id))

## INTRODUCTION

Cargo barges play a strategic role in marine transportation, particularly in the carriage of bulk materials, construction components, heavy equipment, and project cargo in coastal and inland waters [1]. Container transport by barge, commonly referred to as Container on Barge (COB), reduces the cost per TEU, particularly for large-volume shipments over medium to long distances [2]. Owing to their relatively simple hull configuration, large deck area, and high loading flexibility, barges are widely used in operations that require efficient transport of heavy and voluminous cargo [3]. Nevertheless, such operational flexibility also introduces structural challenges, especially with respect to the longitudinal response of the hull girder [4]. Variations in cargo arrangement, loading intensity, and the position of concentrated deck loads may significantly alter the longitudinal distribution of weight, thereby affecting the balance between weight and buoyancy along the vessel's length [5]. If not properly evaluated, these variations may induce excessive internal loads that compromise structural safety and operational reliability.

Longitudinal strength constitutes one of the most essential aspects in the structural assessment of ships and barges, as it reflects the capability of the hull girder to resist global loads acting over the vessel length [6,7]. In practice, the global structural response of a floating body is governed by the interaction between distributed weight and buoyancy, which generates shear force and bending moment [8]. Among these parameters, shear force and still water bending moment are commonly employed as principal indicators for evaluating whether the structural response remains within allowable limits prescribed by classification rules. Accordingly, longitudinal strength

assessment under representative loading scenarios is indispensable to ensure that the vessel can safely withstand operational load variations without exceeding permissible structural boundaries [9].

Previous studies on marine structural analysis have consistently demonstrated that loading configuration has a substantial influence on hull girder behavior. Longitudinal strength investigations generally emphasize the determination of load distribution, shear force, and bending moment along the ship length, followed by comparison with allowable values established by relevant classification societies [10]. Earlier works have also indicated that the most critical structural condition is not always associated with the fully loaded state; in many cases, partial loading conditions, asymmetric cargo placement, or concentrated deck loads may produce more severe local or global responses [11]. This indicates that the structural adequacy of a barge cannot be reliably represented by a single loading case alone, but should instead be evaluated through a set of operationally relevant scenarios [12].

Despite the extensive discussion on longitudinal strength in ship structural design, practical case-based analyses for cargo barges remain highly relevant, particularly for barges subjected to variable deck loading and movable heavy equipment [13]. In actual operation, a cargo barge may experience substantial changes in longitudinal loading pattern due not only to differences in cargo quantity but also to the repositioning of concentrated loads such as deck cranes [14]. These changes can shift the locations and magnitudes of peak shear force and bending moment, thereby affecting the identification of the critical condition for structural assessment [15]. Therefore, an evaluation framework that incorporates multiple realistic loading conditions is necessary to provide a more representative understanding of barge longitudinal behavior in service [16].

The present study examines a cargo barge with principal dimensions of 330 ft × 90 ft × 21 ft and a lightship weight of 1802.9 tons. The assessment considers six loading conditions, namely the lightship condition, fully loaded condition, partially loaded condition at 50% capacity, and three crane-shift configurations representing aft, mid, and fore positions. The analysis is conducted by determining the longitudinal load distribution and evaluating the resulting shear force and still water bending moment along the hull, which are then compared with the permissible limits specified in the applicable classification rules. The available calculation report shows that the study identifies the maximum shear force and still water bending moment for each load case, thereby providing a sound basis for examining the influence of loading variation on hull girder performance.

Based on the above considerations, this study aims to evaluate the longitudinal strength of a cargo barge under various loading conditions by using shear force and still water bending moment as the main assessment parameters. The contribution of this study lies in the systematic evaluation of several realistic operational scenarios, including the effect of crane position shifts, in order to identify the most critical loading condition and its corresponding location along the hull. The results are expected to provide practical insight for designers, operators, and surveyors in assessing barge structural safety and supporting compliance with classification rule requirements.

## METHODS

### Research Object and Data Acquisition

The object of this study is a cargo barge with principal dimensions of 330 ft in length overall, 90 ft in breadth, and 21 ft in depth, with a lightship weight of 1802.9 tons. The longitudinal strength of the barge is evaluated under several representative loading conditions to determine the global hull girder response in terms of shear force and still water bending moment [17]. The research data were obtained from the vessel longitudinal strength calculation report, which includes general particulars, weight components, hydrostatic data, load distribution, permissible structural limits, and the calculated responses for each loading condition [18]. The report also presents frame-based longitudinal distribution data, which form the basis for evaluating internal force variation along the hull.

### Research Variables and Loading Variations

The fixed variables in this study are the principal dimensions of the barge, the hull configuration, the frame-based interval system, and the permissible structural criteria used for evaluation. The response variables are the longitudinal shear force and still water bending moment along the hull girder. The independent variable is the loading condition applied to the vessel. Six loading cases are considered, namely: (1) lightship condition, (2) fully loaded condition, (3) partially loaded condition at 50% cargo load, (4) crane shifted to aft position at Frame 10, (5) crane shifted to mid position at Frame 27, and (6) crane shifted to fore position at Frame 41. These loading variations were selected because they represent realistic operational conditions that may alter the longitudinal load distribution and thus affect the structural response of the barge.

### Method of Analysis

The longitudinal strength evaluation was conducted using a conventional still-water load analysis based on the difference between weight distribution and buoyancy distribution along the vessel length [19]. In this method, the

hull is divided into a number of longitudinal intervals corresponding to frame positions. The distributed load acting on each interval is determined from the total weight per unit length and the buoyancy per unit length [20].

The distributed weight per unit length is expressed as

$$\omega(x) = \frac{W_i}{\Delta x} \quad (1)$$

where  $w(x)$  is the weight distribution at longitudinal position  $x(t/m)$ ,  $W_i$  is the total weight in interval  $i(t)$ , and  $\Delta x$  is the length of the interval (m).

Similarly, the buoyancy distribution per unit length is written as

$$b(x) = \frac{B_i}{\Delta x} \quad (2)$$

where  $b(x)$  is the buoyancy distribution (t/m), and  $B_i$  is the buoyancy force acting within interval  $i(t)$  [21]. The net load distribution along the hull is then obtained from the difference between weight and buoyancy:

$$q(x) = \omega(x) - b(x) \quad (3)$$

where  $q(x)$  is the net load distribution (t/m). A positive value of  $q(x)$  indicates that the local weight exceeds buoyancy, whereas a negative value indicates that buoyancy exceeds weight.

## Research Procedure

The study was carried out through several sequential stages. First, the principal particulars, lightship weight, hydrostatic characteristics, and load case definitions were identified from the available calculation report. Second, the vessel was evaluated under six representative loading conditions consisting of lightship, fully loaded, partially loaded, and three crane-shift scenarios. Third, the longitudinal weight distribution for each load case was arranged according to the frame-based interval system. Fourth, the buoyancy distribution along the hull was determined and compared with the weight distribution to produce the net load curve. Fifth, the net load distribution was integrated to obtain the shear force distribution, and the resulting shear force curve was further integrated to determine the still water bending moment distribution. Finally, the maximum values obtained from each load case were compared with the permissible limits in order to identify the critical condition and evaluate the longitudinal structural adequacy of the cargo barge.

## Tools and Materials

The primary material used in this study is the longitudinal strength calculation report of the cargo barge, which contains the vessel particulars, hydrostatic data, weight distribution, load case arrangement, and longitudinal response results. The analytical basis is the permissible shear force and still water bending moment criteria adopted from the relevant BKI Rules for longitudinal strength. The main tools used in the study consist of the calculation data set, tabulated load distribution results, and frame-based response outputs used to examine the variation of structural behavior under each loading condition.

The permissible shear force and still water bending moment limits used in this study were adopted from the applicable BKI Rules for longitudinal strength assessment. Therefore, the structural acceptability of the barge was evaluated by comparing the calculated maximum shear force and still water bending moment with the allowable rule-based values. In this study, all weight-related quantities expressed in tons refer to metric tons, unless otherwise stated.

The partially loaded condition at 50% cargo capacity was modelled as a homogeneously distributed cargo load along the designated cargo deck region. This assumption was applied to represent an intermediate operational loading condition without intentional longitudinal concentration at the aft, midship, or fore region.

## Weight Distribution, Loading, Shearing Force and Bending Moment Weight Distribution

The longitudinal weight distribution was determined by subdividing the vessel into a series of longitudinal intervals along the hull. In the present study, the barge was divided into 106 displacement intervals, following the arrangement available in the longitudinal strength calculation report. For each interval, the weight contribution of every structural component, outfit item, machinery component, and payload element was assigned according to its longitudinal extent and center of gravity [22]. The total weight within each interval was then divided by the corresponding interval length to obtain the mean distributed weight per unit length [23]. This procedure is commonly adopted in longitudinal strength assessment because it enables the transformation of discrete shipboard weights into a continuous load representation along the vessel length. To preserve the physical consistency of the

loading model, the longitudinal center of gravity of each item was checked after distribution so that the overall center of gravity of the vessel remained consistent with the original loading data.

### Loading, Shearing Force and Bending Moment

After the longitudinal weight distribution had been established, it was compared with the buoyancy distribution along the vessel length to determine the net load acting on the hull girder. The buoyancy curve was arranged over the same longitudinal intervals so that the difference between the distributed weight and distributed buoyancy in each interval represented the net loading intensity [24]. In still-water longitudinal strength analysis, this net loading forms the basis for calculating the shear force and bending moment along the hull [25].

The net load for each interval is expressed as:

$$q_i = \omega(i) - b(i) \quad (4)$$

where  $q_i$  is the net load intensity (t/m),  $w_i$  is the distributed weight (t/m), and  $b_i$  is the distributed buoyancy (t/m). A positive value of  $q_i$  indicates that weight exceeds buoyancy in the interval, while a negative value indicates that buoyancy exceeds weight.

The shear force distribution was then obtained by integrating the net load curve from one end of the vessel to the other. In the discrete interval-based approach, this integration is performed by cumulative summation of the net load over successive intervals:

$$V_i = V_{i-1} + q_i \Delta x_i \quad (5)$$

where  $V_i$  is the shear force at the end of interval  $i$  (t),  $V_{i-1}$  is the shear force at the preceding interval, and  $q_i \Delta x_i$  is the incremental vertical load contribution. According to longitudinal strength theory, the final shear force at the opposite end of the hull should ideally return to zero as a consequence of overall vertical equilibrium. In practice, however, a small residual value may appear due to rounding and discretization errors. This residual is commonly corrected by distributing the error proportionally along the baseline so that the corrected shear force curve satisfies end equilibrium. Such treatment is consistent with standard longitudinal strength calculation procedures used in ship structural assessment.

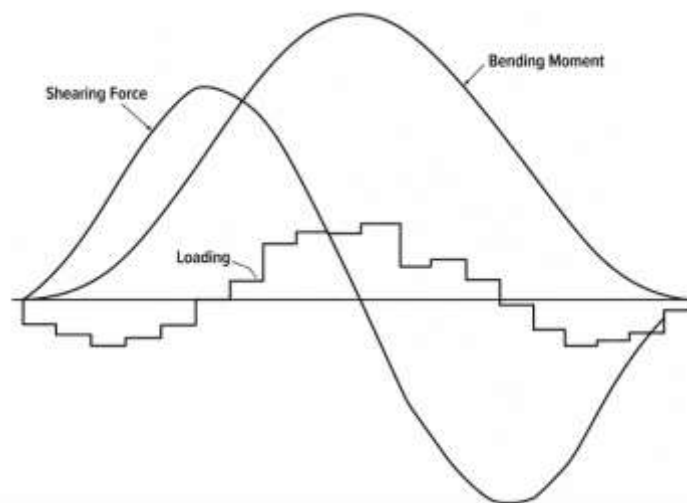


**Figure 1.** Typical loading, shearing force and bending moment curves

The typical loading curve shown in Figure 1 illustrates the longitudinal relationship between the distributed weight and buoyancy along the vessel, where their difference forms the net loading acting on the hull girder. In the midship region, buoyancy generally exceeds weight, producing an upward net load, while in the end regions the distributed weight may exceed buoyancy, producing downward net loads [26]. This net loading distribution is then integrated along the ship length to obtain the shearing force curve, which changes progressively according to the cumulative effect of the applied loads. A further integration of the shearing force curve yields the bending moment curve, which represents the global longitudinal bending response of the hull girder. Therefore, the figure demonstrates the fundamental sequence of longitudinal strength analysis, namely that the loading distribution governs the shearing force distribution, and the shearing force distribution in turn governs the bending moment distribution [27].

## RESULTS AND DISCUSSION

### Loading Conditions and Longitudinal Load Distribution General particulars of the barge

The object evaluated in this study is a cargo barge with principal dimensions of 330 ft in length overall, 90 ft in breadth, and 21 ft in depth. The barge has a lightship weight of 1802.9 tons, representing the structural and outfit weight of the vessel before the addition of cargo and other operational loads. These principal particulars provide the basic geometric and weight characteristics required for longitudinal strength assessment, since the vessel dimensions and lightship condition directly influence the longitudinal distribution of weight, buoyancy, and the resulting hull girder response.

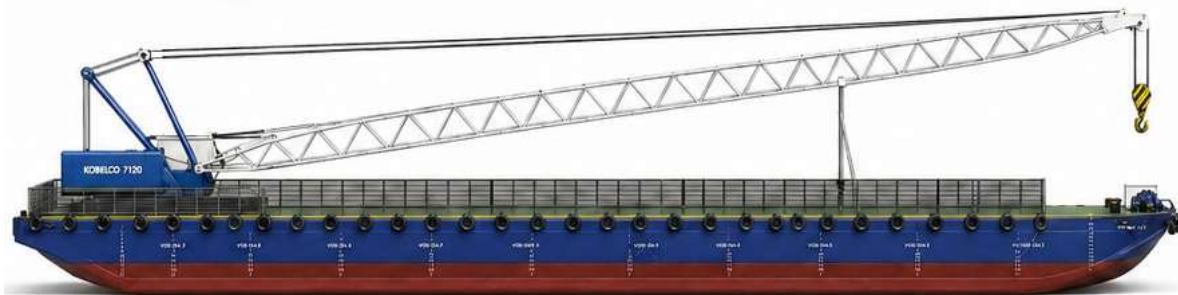


**Figure 2.** General particulars of the barge

As a wide-deck cargo barge, the vessel is intended to accommodate substantial loading variations along its length, making it necessary to evaluate its structural behavior under several representative loading conditions.

### List of loading conditions

To evaluate the longitudinal strength of the cargo barge under representative operational scenarios, six loading conditions were considered: lightship, fully loaded, partially loaded (50%), and three crane-shift positions (aft, mid, fore). These cases capture variations in cargo magnitude and the effect of concentrated load relocation along the vessel length, which significantly influences the distribution of net load, shear force, and still water bending moment along the hull girder. The lightship condition represents the baseline structural weight without cargo, while the fully and partially loaded conditions reflect primary operational scenarios. The crane-shift cases assess the impact of deck load relocation on longitudinal structural response. Overall, these six cases provide a comprehensive representation of actual operating conditions and help identify the most critical scenario for longitudinal strength assessment.

**Table 1.** Loading conditions considered in the longitudinal strength assessment

Load Case	Loading Condition	Description
LC1	Lightship condition	Barge in lightship condition without cargo load, representing the basic structural weight distribution of the vessel.
LC2	Fully loaded 100%	Barge under full cargo loading condition, representing the maximum operational loading case.
LC3	Partially loaded 50%	Barge under partial cargo loading, representing an intermediate operational condition between lightship and full load.
LC4	Crane shift to aft position (Fr. 10)	Loading condition with the crane positioned near the aft region at Frame 10 to evaluate the effect of aft concentrated load placement.
LC5	Crane shift to mid position (Fr. 27)	Loading condition with the crane positioned near the midship region at Frame 27 to examine the structural response under central concentrated loading.
LC6	Crane shift to fore position (Fr. 41)	Loading condition with the crane positioned near the fore region at Frame 41 to assess the influence of forward concentrated load placement.

### Equilibrium data for each load case

Equilibrium data for each load case were used to define the total loading condition of the barge before deriving the longitudinal load distribution. For each loading case, the equilibrium table provides the mass of each loading component together with its longitudinal, transverse, and vertical arm, allowing the overall weight and center of gravity of the vessel to be determined. In the lightweight condition, the total loadcase was 1802.990 tonnes with a longitudinal arm of 43.620 m and a vertical arm of 4.493 m. In the fully loaded condition, the addition of deck cargo amounting to 10600.000 tonnes increased the total loadcase to 12402.990 tonnes, with a longitudinal arm of 47.192 m and a vertical arm of 8.541 m. These equilibrium data form the basis for establishing the longitudinal weight distribution for each operational scenario and are therefore essential in the subsequent calculation of net load, shear force, and still water bending moment.

### Load distribution table for each load case

The load distribution table for each load case was used to describe the longitudinal variation of the applied load along the hull girder. The table presents the longitudinal position together with the distributed mass, buoyancy, grounding, damage or net buoyancy variation, net load, shear force, and bending moment. In the context of the present subsection, the most relevant parameters are the distributed mass, distributed buoyancy, and resulting net load, since these quantities define the longitudinal loading pattern of the barge. The net load at each interval is obtained from the difference between the mass distribution and buoyancy distribution, thereby indicating whether a particular region is dominated by downward weight or upward buoyant support. For the lightweight condition, the load distribution extends continuously from the aft end to the forward end of the vessel, with changing values of mass and buoyancy along the hull that produce a varying net load profile. This profile forms the fundamental basis for the subsequent derivation of shear force and still water bending moment distributions under each loading condition.

Figure 3 illustrates the longitudinal distribution of mass, buoyancy, net load, shear force, and bending moment along the barge length for the evaluated loading condition. The difference between the mass and buoyancy curves produces the net load distribution, which varies along the hull according to the local balance between downward weight and upward buoyant support. This net load is then integrated to obtain the shear force curve, while further integration of the shear force yields the bending moment curve. The figure shows that changes in the longitudinal loading pattern directly influence the magnitude and location of the resulting internal forces, thereby providing the basis for identifying the critical structural response of the hull girder.

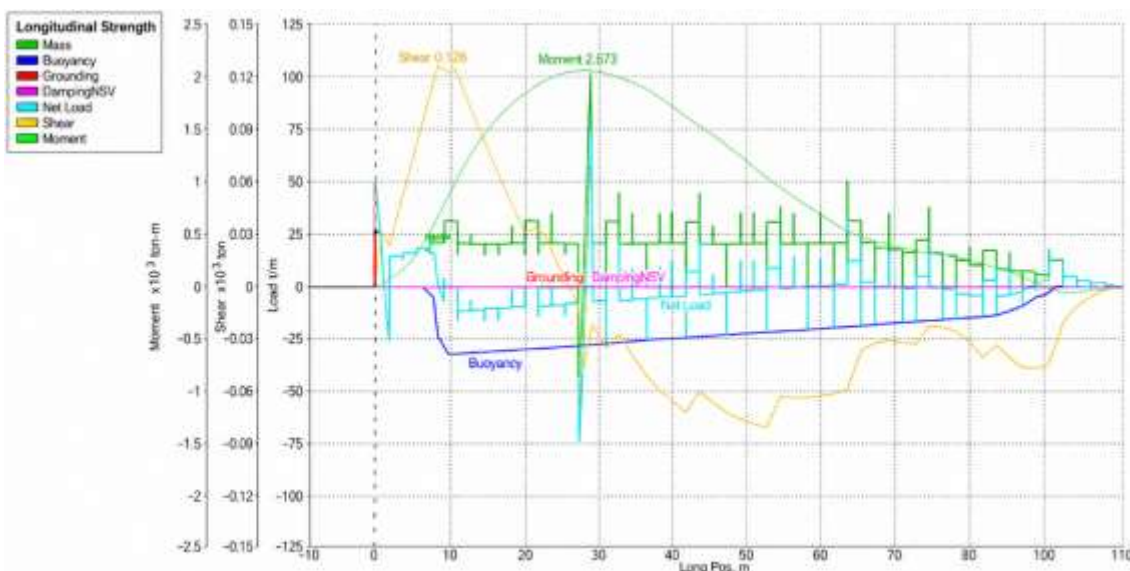


**Figure 3.** Illustrates the longitudinal distribution of mass, buoyancy, net load, shear force, and bending moment along the barge length for the evaluated loading condition

Based on the longitudinal load distribution described above, the next step of the analysis is to examine the resulting shear force distribution in order to identify the critical locations and the maximum shear force generated under each loading condition.

## Shear Force Results

The maximum shear force obtained under each loading condition is summarized in Table 2. The results show that the shear force response of the barge varies with changes in cargo magnitude and the longitudinal position of concentrated loads. In general, the fully loaded condition produced the highest shear force, while the lightship condition resulted in the lowest value. The variation in the location of the maximum shear force also indicates that load redistribution along the hull influences the critical frame position.

**Table 2.** Maximum shear force under various loading conditions

Load Case	Loading Condition	Maximum Shear Force ( $\times 10^3$ ton)	Critical Location
LC1	Lightship condition	0.126	Fr. 6
LC2	Fully loaded 100%	0.385	Fr. 50
LC3	Partially loaded 50%	0.24	Fr. 5
LC4	Crane shift to aft position	0.196	Fr. 10
LC5	Crane shift to mid position	0.172	Fr. 6
LC6	Crane shift to fore position	0.179	Fr. 6

The increase in shear force under LC2 is physically related to the larger imbalance between downward cargo weight and upward buoyancy along the hull length. In the fully loaded condition, the distributed cargo load increases the cumulative vertical force, resulting in the highest shear force among all evaluated cases. Although the crane-shift cases introduced concentrated load effects, their total loading magnitude was lower than the fully loaded case; therefore, the resulting shear force remained less critical. This indicates that, for the present barge configuration, the total cargo magnitude has a stronger influence on the global shear response than crane relocation alone.

As shown in Table 2, LC2 (fully loaded) produced the highest shear force,  $0.385 \times 10^3$  ton at Frame 50, indicating the most critical internal force due to increased imbalance between weight and buoyancy. In contrast, LC1 (lightship) yielded the lowest value,  $0.126 \times 10^3$  ton at Frame 6, reflecting minimal load. LC3 (partially loaded) reached  $0.240 \times 10^3$  ton at Frame 5, confirming that moderate cargo significantly increases shear response. Crane-shift conditions (LC4–LC6) produced  $0.196 \times 10^3$  ton,  $0.172 \times 10^3$  ton, and  $0.179 \times 10^3$  ton, respectively. While load relocation slightly shifted the critical frame (notably LC4 at Frame 10), their effects remained less significant than full cargo loading.

When compared with the permissible shear force given in the report, all calculated values remained below the allowable limit, indicating that the barge satisfies the still-water shear force requirement for all investigated loading conditions. Overall, the results demonstrate that the fully loaded condition governs the shear force response of the vessel, whereas the lightship condition represents the least critical case.

## Still Water Bending Moment Results

The maximum still water bending moment obtained for each loading condition is summarized in Table 3. The results indicate that the bending moment response of the barge varies considerably with the applied loading scenario. In contrast to the shear force response, the most critical bending moment occurred in the fully loaded condition with a negative value, indicating a dominant sagging tendency. Meanwhile, the other loading conditions generally produced positive bending moments, indicating hogging behavior at their respective critical sections.

**Table 3.** Maximum still water bending moment under various loading conditions

Load Case	Loading Condition	Maximum SWBM ( $\times 10^3$ ton-m)	Critical Location
LC1	Lightship condition	2.043	Fr. 16
LC2	Fully loaded 100%	-6.212	Fr. 35
LC3	Partially loaded 50%	3.178	Fr. 14
LC4	Crane shift to aft position	2.877	Fr. 20
LC5	Crane shift to mid position	1.89	Fr. 14
LC6	Crane shift to fore position	2.394	Fr. 18

As shown in Table 3, LC2 (fully loaded condition) produced the most critical still water bending moment, namely  $-6.212 \times 10^3$  ton-m at Frame 35. The negative sign indicates that the hull girder experienced a dominant sagging moment under this loading condition. This result suggests that the full cargo load generated the greatest longitudinal bending demand, particularly in the midship region where the effect of distributed cargo weight became most significant relative to buoyancy support.

In contrast, LC1 (lightship condition) resulted in a positive still water bending moment of  $2.043 \times 10^3$  ton·m at Frame 16, indicating a relatively moderate hogging response. The lighter loading arrangement in this condition reduced the longitudinal bending demand compared with the cargo-carrying cases. For LC3 (partially loaded 50%), the bending moment increased to  $3.178 \times 10^3$  ton·m at Frame 14, which shows that partial cargo loading was sufficient to raise the global bending response, although it remained less severe than the fully loaded condition in absolute magnitude.

The crane-shift conditions also affected the still water bending moment, with LC4, LC5, and LC6 producing maximum values of  $2.877 \times 10^3$  ton·m,  $1.890 \times 10^3$  ton·m, and  $2.394 \times 10^3$  ton·m, respectively. These values indicate that the relocation of the crane modified the bending response of the hull girder, but the resulting moments were still smaller in magnitude than that of the fully loaded condition. Among the crane-shift cases, the aft crane position in LC4 generated the highest bending moment, suggesting that aft concentration of load had a more pronounced influence on longitudinal bending than the midship and fore crane positions.

When compared with the permissible still water bending moment given in the report, all calculated values remained below the allowable limit, indicating that the barge satisfies the still-water bending moment requirement for all investigated loading conditions. Overall, the results show that the fully loaded condition governs the global bending response of the vessel, while the crane-shift conditions mainly produce moderate variations in moment magnitude and critical location.

The maximum still water bending moment obtained for each loading condition is summarized in Table 3. The results indicate that the bending moment response of the barge varies considerably with the applied loading scenario. The most critical bending moment occurred in LC2, where the negative still water bending moment indicates a dominant sagging condition. In hull girder behavior, sagging generally occurs when the downward loading effect in the midship region becomes dominant relative to buoyancy support, causing the hull girder to bend downward in the middle. In contrast, the positive bending moments observed in the other loading cases indicate a tendency toward hogging behavior at their respective critical locations.

The governing sagging response in LC2 confirms that the fully loaded condition is the most demanding case for longitudinal bending. The maximum still water bending moment of  $-6.212 \times 10^3$  metric ton·m at Frame 35 reached 33.58% of the permissible bending moment limit. This utilization level demonstrates that, although LC2 governs the bending response, the barge still retains a substantial structural margin under still-water conditions.

### Comparison with Permissible Limits

To assess the structural adequacy of the barge, the maximum shear force and still water bending moment obtained from each loading condition were compared with the permissible limits specified in the longitudinal strength calculation report. The report gives the permissible shear force as +1185 ton and -1165 ton, and the permissible still water bending moment as +18500 ton·m and -18500 ton·m over the main longitudinal strength region. These allowable values were used as the reference for evaluating whether the calculated responses remained within acceptable structural limits.

**Table 4.** Comparison of calculated responses with permissible limits

Load Case	Loading Condition	Max. Shear Force ( $\times 10^3$ ton)	Shear Utilization (%)	Max. SWBM ( $\times 10^3$ ton·m)	SWBM Utilization (%)	Structural Status
LC1	Lightship condition	0.126	10.63	2.043	11.04	Acceptable
LC2	Fully loaded 100%	0.385	32.49	-6.212	33.58	Acceptable
LC3	Partially loaded 50%	0.24	20.25	3.178	17.18	Acceptable
LC4	Crane shift to aft position	0.196	16.54	2.877	15.55	Acceptable
LC5	Crane shift to mid position	0.172	14.51	1.89	10.22	Acceptable
LC6	Crane shift to fore position	0.179	15.11	2.394	12.94	Acceptable

As presented in Table 4, all calculated shear force and still water bending moment values remained well below the permissible limits. This indicates that the barge satisfies the longitudinal strength requirement for all evaluated loading conditions. The highest utilization was observed in LC2 (fully loaded condition), which reached 32.49% of the allowable shear force and 33.58% of the allowable still water bending moment. Although this condition produced the most severe structural response, the calculated values were still substantially lower than the permissible limits, indicating that a sufficient structural safety margin was maintained.

The remaining loading conditions exhibited lower utilization levels, with lightship and crane-shift cases generally producing moderate responses. This suggests that the barge has adequate longitudinal strength not only under baseline and partial loading conditions but also under operational scenarios involving relocation of a concentrated deck load. From an engineering perspective, these results confirm that the hull girder response remains within acceptable rule-based limits throughout all investigated loading cases, and no condition indicates an immediate risk of exceeding the allowable still-water structural capacity.

Overall, the comparison with permissible limits demonstrates that the vessel is structurally acceptable under all investigated loading conditions. Nevertheless, the fully loaded condition should be regarded as the governing case for operational consideration, since it consistently produced the highest shear force and bending moment utilization among all scenarios evaluated.

It should be noted that the present assessment is limited to still-water longitudinal strength analysis. The calculated shear force and bending moment were obtained from the equilibrium between the longitudinal distribution of weight and buoyancy under calm-water loading conditions. Therefore, the “Acceptable” status reported in this study refers specifically to the still-water loading scenarios evaluated in the calculation. Wave-induced bending moments, dynamic sea loads, and combined still-water and wave-induced longitudinal strength effects were not included in the present analysis. Consequently, the results should be interpreted as a rule-based still-water strength assessment rather than a complete seagoing strength evaluation under actual wave conditions.

### Critical Condition and Discussion

Based on the comparison of all loading cases, the fully loaded condition (LC2) was identified as the most critical operating scenario for the cargo barge. This condition produced both the highest maximum shear force, equal to  $0.385 \times 10^3$  ton at Frame 50, and the largest absolute value of still water bending moment, equal to  $-6.212 \times 10^3$  ton-m at Frame 35. These results indicate that the full cargo arrangement generated the most severe global structural response among all investigated loading conditions. The negative bending moment further shows that the hull girder was predominantly subjected to a sagging condition under this load case[26].

The dominance of LC2 may be attributed to the substantial increase in distributed deck cargo, which significantly altered the balance between weight and buoyancy along the vessel length. In comparison with the lightship and partial loading cases, the fully loaded condition imposed a much greater downward load, thereby increasing both the cumulative shear force and the longitudinal bending demand. This behavior is consistent with the general principle of longitudinal strength, in which the hull girder response is governed by the extent of imbalance between the applied weight distribution and the available buoyant support. Under LC2, this imbalance became more pronounced, especially in the midship-to-forward region, leading to higher internal force accumulation and a more critical bending response.

The lightship condition (LC1), on the other hand, represented the least critical structural response, with the lowest maximum shear force and a relatively moderate positive bending moment. This result reflects the absence of cargo loading and the relatively lighter longitudinal weight distribution of the vessel. The partially loaded case (LC3) produced intermediate values, confirming that even a moderate increase in cargo load was sufficient to raise the hull girder response, although not to the same extent as the fully loaded condition. These findings indicate that the magnitude of cargo load remains the governing factor in determining the overall severity of longitudinal structural response.

The crane-shift conditions (LC4–LC6) provide additional insight into the effect of concentrated load relocation on hull girder behavior. Although none of these cases exceeded the response produced by LC2, the results show that moving the crane along the vessel length changed both the magnitude and the location of the critical internal forces. In particular, the aft crane position (LC4) generated the largest bending moment among the crane-shift cases, while the mid and fore positions produced somewhat lower responses. This suggests that concentrated load placement may locally intensify the longitudinal structural demand, even when the total loading magnitude remains unchanged. Therefore, crane positioning should be considered as an operational factor that can influence the internal load distribution and should not be neglected in longitudinal strength assessment.

From the perspective of structural safety, all evaluated loading conditions remained within the permissible shear force and still water bending moment limits specified in the calculation report. This indicates that the cargo barge possesses sufficient longitudinal strength to withstand the investigated still-water loading scenarios. However, the fact that LC2 consistently produced the highest utilization confirms that the fully loaded condition should be treated as the governing design and operational reference for the vessel. In practical terms, this means that full cargo loading requires the greatest attention during load planning and operational verification, particularly with respect to maintaining an acceptable longitudinal load distribution.

Overall, the present results demonstrate that the longitudinal structural response of the barge is strongly influenced by both the magnitude of cargo loading and the longitudinal position of concentrated deck loads. The study confirms that the most severe response does not arise from crane relocation alone, but from the combined effect of large distributed cargo load and its interaction with buoyancy over the hull length. These findings are

useful for supporting safer loading arrangements and for ensuring that the vessel continues to operate within acceptable structural limits under realistic service conditions.

The criticality of LC2 can be explained by the physical interaction between the longitudinal weight distribution and buoyancy distribution. In the fully loaded condition, the addition of cargo substantially increases the downward load acting along the deck, particularly in the cargo-carrying region. This condition produces a larger imbalance between weight and buoyancy compared with the lightship, partial loading, and crane-shift cases. As a result, the cumulative vertical load becomes greater, leading to the highest shear force of  $0.385 \times 10^3$  metric tons at Frame 50 and the largest absolute still water bending moment of  $-6.212 \times 10^3$  metric ton·m at Frame 35. The negative bending moment indicates a dominant sagging condition, where the hull girder tends to bend downward in the midship region due to the greater downward cargo load relative to buoyant support.

## CONCLUSION

This study evaluated the longitudinal strength of a cargo barge under six representative loading conditions by using shear force and still water bending moment as the main assessment parameters. The results show that the longitudinal structural response of the barge is strongly affected by variations in loading magnitude and the longitudinal position of concentrated loads. Among all investigated cases, the fully loaded condition was identified as the most critical scenario, producing the highest maximum shear force of  $0.385 \times 10^3$  ton at Frame 50 and the largest absolute still water bending moment of  $-6.212 \times 10^3$  ton·m at Frame 35. This indicates that the full cargo arrangement generated the most severe hull girder response and should therefore be regarded as the governing operational condition for longitudinal strength assessment. The study also shows that partial loading and crane-shift conditions modified the magnitude and location of the internal forces, although their responses remained less critical than those of the fully loaded case. The lightship condition produced the lowest shear force and a relatively moderate bending moment, while the crane relocation cases demonstrated that concentrated load positioning can influence the longitudinal internal force distribution even when the total loading level does not change significantly. These findings confirm that both cargo magnitude and load placement play important roles in determining the global structural behavior of the barge. Based on the comparison with the permissible limits specified in the calculation report, all investigated loading conditions remained within the allowable shear force and still water bending moment criteria. This confirms that the cargo barge possesses adequate longitudinal strength under the evaluated still-water loading scenarios and satisfies the applicable structural safety requirements. Overall, the study concludes that the vessel is structurally acceptable for all considered operating conditions, with the fully loaded condition representing the most critical reference case for safe load planning and operational control. This study is limited to the evaluation of longitudinal strength under still-water loading conditions. Wave-induced bending moments, dynamic sea loads, local deck structural responses due to crane movement, and fatigue effects were not included in the present analysis. Future studies should consider combined still-water and wave-induced bending moments, dynamic loading effects, local strength assessment, and finite element-based verification to provide a more comprehensive evaluation of barge structural safety under realistic operating conditions.

## ACKNOWLEDGEMENT

The authors would like to express their sincere appreciation to Politeknik Negeri Bengkalis, Politeknik Negeri Batam, and Universitas Raja Ali Haji for their institutional support and academic collaboration throughout this research. The authors also acknowledge all parties who assisted in providing technical data, calculation reports, and relevant information that supported the completion of this study.

## REFERENCES

- [1] P. Yanakiev, Y. Garbatov, and P. Georgiev, "Advances of Articulated Tug–Barge Transport in Enhancing Shipping Efficiency," *J. Mar. Sci. Eng.*, vol. 13, no. 8, p. 1451, Jul. 2025, doi: [10.3390/jmse13081451](https://doi.org/10.3390/jmse13081451).
- [2] F. Bu and H. Nachtmann, "Literature review and comparative analysis of inland waterways transport: 'Container on Barge,'" *Maritime Economics & Logistics*, vol. 25, no. 1, pp. 140–173, Mar. 2023, doi: [10.1057/s41278-021-00195-6](https://doi.org/10.1057/s41278-021-00195-6).
- [3] B. Duldner-Borca, L. Hoerandner, B. Bieringer, R. Khanbilverdi, and L.-M. Putz-Egger, "New Design Options for Container Barges with Improved Navigability on the Danube," *Sustainability*, vol. 16, no. 11, p. 4613, May 2024, doi: [10.3390/su16114613](https://doi.org/10.3390/su16114613).

- [4] C. H. Jang and D. K. Kim, "An advanced technique to adjust hull girder load: Part 1 = generalisation," *International Journal of Naval Architecture and Ocean Engineering*, vol. 17, p. 100645, 2025, doi: [10.1016/j.ijnaoe.2025.100645](https://doi.org/10.1016/j.ijnaoe.2025.100645).
- [5] J. Abedin, F. Franklin, and S. M. I. Mahmud, "Linear Longitudinal Strength Analysis of a Multipurpose Cargo Ship under Combined Bending and Torsional Load," *J. Mar. Sci. Eng.*, vol. 12, no. 1, p. 59, Dec. 2023, doi: [10.3390/jmse12010059](https://doi.org/10.3390/jmse12010059).
- [6] R. Adiputra, T. Yoshikawa, and E. Erwandi, "Reliability-based assessment of ship hull girder ultimate strength," *Curved and Layered Structures*, vol. 10, no. 1, Feb. 2023, doi: [10.1515/cls-2022-0189](https://doi.org/10.1515/cls-2022-0189).
- [7] Alamsyah A, Nurcholik SD, Suardi S, Pawarah MU, Jumalia J. The strength and fatigue life analysis of sedan car ramp of the ferry Ro-Ro 5000 GT using finite element method. *Kapal: Jurnal Ilmu Pengetahuan dan Teknologi Kelautan*. 2021 Jun 14;18(2):101-10. doi: [10.14710/kapal.v18i2.37518](https://doi.org/10.14710/kapal.v18i2.37518)
- [8] H. Yu, S. Wu, Y. Zhao, W. Liu, and H. Yang, "A Novel Hull Girder Design Methodology for Prediction of the Longitudinal Structural Strength of Ships," *J. Mar. Sci. Eng.*, vol. 12, no. 12, p. 2368, Dec. 2024, doi: [10.3390/jmse12122368](https://doi.org/10.3390/jmse12122368).
- [9] N. Ilić and N. Momčilović, "Evaluation of hull girder ultimate strength for dry cargo inland vessels," *Marine Structures*, vol. 102, p. 103790, Jul. 2025, doi: [10.1016/j.marstruc.2025.103790](https://doi.org/10.1016/j.marstruc.2025.103790).
- [10] S. K. Prabu Chelladurai, A. K. Dash, V. Nagarajan, and O. P. Sha, "Longitudinal strength of high block coefficient merchant ships in irregular waves," *Ocean Engineering*, vol. 283, p. 115066, Sep. 2023, doi: [10.1016/j.oceaneng.2023.115066](https://doi.org/10.1016/j.oceaneng.2023.115066).
- [11] S. P. Selvia, R. W. Prastianto, and Murdjito, "Longitudinal strength analysis of a crane barge during heavy lifting operation due to variations of trim," *IOP Conf. Ser. Earth Environ. Sci.*, vol. 1473, no. 1, p. 012003, Mar. 2025, doi: [10.1088/1755-1315/1473/1/012003](https://doi.org/10.1088/1755-1315/1473/1/012003).
- [12] B. Jingga, Y. Yuan, L. Guoa, and W. Tang, "Stress Reconstruction Method for an Ore Carrier Based on Multi-Level Structural Response Fields," *e-Journal of Nondestructive Testing*, vol. 31, no. 2, Feb. 2026, doi: [10.58286/32478](https://doi.org/10.58286/32478).
- [13] D. Xiang, Y. Yu, and X. Gao, "A numerical critical shear crack model and its application to post- peak behavior assessment of <sc>RC</sc> and <sc>SFRC</sc> beams," *Structural Concrete*, vol. 25, no. 4, pp. 2800–2818, Aug. 2024, doi: [10.1002/suco.202300863](https://doi.org/10.1002/suco.202300863).
- [14] Y. B. Hadasa, Murdjito, R. W. Prastianto, E. B. Djatmiko, Wahyudi, and M. Faiz, "Study on the effects of lifting loads on the longitudinal strength of a crane barge during heavy lifting operations due to various angle of crane rotation," *IOP Conf. Ser. Earth Environ. Sci.*, vol. 1298, no. 1, p. 012021, Feb. 2024, doi: [10.1088/1755-1315/1298/1/012021](https://doi.org/10.1088/1755-1315/1298/1/012021).
- [15] M. Parulian, N. Nurmawati, and A. Dianiswara, "Stability And Longitudinal Strength Analysis On Barge 400 Ft During Sea Transportation Decommissioning Jacket," *Wave: Jurnal Ilmiah Teknologi Maritim*, vol. 18, no. 2, pp. 91–98, Dec. 2024, doi: [10.55981/wave.2024.1910](https://doi.org/10.55981/wave.2024.1910).
- [16] N. A. Papadopoulos, M. C. Naoum, G. M. Sapidis, and C. E. Chalioris, "Cracking and Fiber Debonding Identification of Concrete Deep Beams Reinforced with C-FRP Ropes against Shear Using a Real-Time Monitoring System," *Polymers (Basel)*, vol. 15, no. 3, p. 473, Jan. 2023, doi: [10.3390/polym15030473](https://doi.org/10.3390/polym15030473).
- [17] T. Putranto, M. Körgesaar, and K. Tabri, "Application of Equivalent Single Layer Approach for Ultimate Strength Analyses of Ship Hull Girder," *J. Mar. Sci. Eng.*, vol. 10, no. 10, p. 1530, Oct. 2022, doi: [10.3390/jmse10101530](https://doi.org/10.3390/jmse10101530).
- [17] D. Li and Z. Chen, "Advanced empirical formulae for the ultimate strength assessment of continuous hull plate under combined biaxial compression and lateral pressure," *Eng. Struct.*, vol. 285, p. 116041, Jun. 2023, doi: [10.1016/j.engstruct.2023.116041](https://doi.org/10.1016/j.engstruct.2023.116041).

- [18] A. I. Wulandari, Suardi, Alamsyah, and A. Ciptiandi, "Strength Analysis with Variation of Construction Transverse Watertight Bulkhead On Ship Container 8842 DWT Using Finite Element Method", *IJMEIR*, vol. 8, no. 2, pp. 109–116, Jul. 2025. doi: <https://doi.org/10.12962/j25481479.v8i2>
- [19] M. Moshref-Javadi and M. Gandomkar, "Investigating the Effects of Cargo Weight and its Distribution on the Dynamic Performance of a High-Speed Planing Hull," *Pomorstvo*, vol. 38, no. 1, pp. 30–42, Jun. 2024, doi: [10.31217/p.38.1.3](https://doi.org/10.31217/p.38.1.3).
- [20] M. Chillemi, F. Cucinotta, and F. Sfravara, "Numerical Analysis and Geometric Assessment of Air Layer Distribution in a Ventilated Planing Hull in Calm Water," *Journal of Marine Science and Application*, vol. 25, no. 1, pp. 46–62, Feb. 2026, doi: [10.1007/s11804-025-00685-6](https://doi.org/10.1007/s11804-025-00685-6).
- [21] N. Zhao, B.-Q. Chen, Y.-Q. Zhou, Z.-J. Li, J.-J. Hu, and C. Guedes Soares, "Experimental and numerical investigation on the ultimate strength of a ship hull girder model with deck openings," *Marine Structures*, vol. 83, p. 103175, May 2022, doi: [10.1016/j.marstruc.2022.103175](https://doi.org/10.1016/j.marstruc.2022.103175).
- [22] Y. B. Hadasa, Murdjito, R. W. Prastianto, E. B. Djatmiko, Wahyudi, and M. Faiz, "Study on the effects of lifting loads on the longitudinal strength of a crane barge during heavy lifting operations due to various angle of crane rotation," *IOP Conf. Ser. Earth Environ. Sci.*, vol. 1298, no. 1, p. 012021, Feb. 2024, doi: [10.1088/1755-1315/1298/1/012021](https://doi.org/10.1088/1755-1315/1298/1/012021).
- [23] J. P. Quispe, S. F. Estefen, M. I. Lourenço, J. H. Chujutalli, and T. Gurova, "Numerical analysis of residual longitudinal strength of a small-scale hull box girder under damage and bending moment," *Marine Systems & Ocean Technology*, vol. 20, no. 1, p. 11, Mar. 2025, doi: [10.1007/s40868-024-00157-6](https://doi.org/10.1007/s40868-024-00157-6).
- [24] M. Ibrahim and M. Soliman, "Reliability quantification and ultimate capacity analysis of ship hulls subjected to cyclic bending moments," *Structure and Infrastructure Engineering*, vol. 21, no. 11–12, pp. 2083–2100, Dec. 2025, doi: [10.1080/15732479.2025.2560049](https://doi.org/10.1080/15732479.2025.2560049).
- [25] S. Li, Z. Hu, and S. Benson, "Progressive collapse analysis of ship hull girders subjected to extreme cyclic bending," *Marine Structures*, vol. 73, p. 102803, Sep. 2020, doi: [10.1016/j.marstruc.2020.102803](https://doi.org/10.1016/j.marstruc.2020.102803).
- [26] R. Adiputra, T. Yoshikawa, and E. Erwandi, "Reliability-based assessment of ship hull girder ultimate strength," *Curved and Layered Structures*, vol. 10, no. 1, Feb. 2023, doi: [10.1515/cls-2022-0189](https://doi.org/10.1515/cls-2022-0189).
- [27] M. K. Rizki, P. Y. Arianto, S. Sumarji, and R. Rudianto, "Strength Analysis of Deck A KM. Dharma Kencana V Due to The Addition of Construction With The Finite Element Method," *Indonesian Journal of Maritime Technology*, vol. 3, no. 2, Nov. 2025, doi: [10.35718/ismatech.v3i2.8481374](https://doi.org/10.35718/ismatech.v3i2.8481374).